Magazine of Civil Engineering

ISSN 2712-8172

journal homepage: http://engstroy.spbstu.ru/

Research article

UDC 624

DOI: 10.34910/MCE.127.9

The roughness and bumping model for cement pavement in seasonal frost regions

H.Q. Li[1], ***Q. Sun***[2]✉, ***I.Z. Ideris***[2], ***Q.Q. Zhao***[3], ***R.S. Fediuk***[4], ***Y.C. Lei***[5], ***Y.Z. Yang***[3]

[1] *CHELBI Engineering Consultants Inc., Beijing, China*

[2] *Infrastructure University Kuala Lumpur, Kuala Lumpur, Malaysia*

[3] *Northeast Agricultural University, Harbin, China*

[4] *Far Eastern Federal University, Vladivostok, Russian Federation*

[5] *Central South University, Changsha, China*

✉ *465390034@qq.com*

Keywords: concrete, pavement management, numerical model, regression analysis

Abstract. The Statistical Package for Social Sciences (SPSS) Statistics software suit was used to test the model's goodness of fit and its normal distribution. Combined with the actual pavement survey data these tools were used to verify the model. The research results show that: permafrost and water-rich conditions have the same effect on pavement roughness and bumping; four key factors, including pavement riding quality index (RQI), pavement bumping index (PBI), frozen soil and water-rich environmental factors have significant impact on pavement roughness and bumping. The prediction model adjusted R^2 is 0.970, which is close to 1. The proposed model provides a high degree of fit and satisfies the assumption of normal distribution. When the PBI is from 87.5 to 95, the permafrost environmental factor is from 0.0002 to 0.0014, and the water-rich environmental factor is from 10.73 to 14.87, the prediction level of the model is the best. The model's RQI prediction value and the measured value has a degree of fit 0.987, which shows a good prediction effect. The prediction model can reasonably predict the roughness and the bumping of cement concrete pavement, which is of great significance to improve road traffic safety and to prolong the service life of cement concrete pavement in seasonal frost regions and water-rich areas.

Funding: Postdoctoral Program of Northeast Agricultural University; Research on the Causes and Early Warning Mechanisms of Longitudinal Cracks on Road Surface under Rich Water Conditions (86010100) Ministry of Education Industry University Research Cooperation Project (86010708)

Citation: Li, H.Q., Sun, Q., Ideris, I.Z., Zhao, Q.Q., Fediuk, R.S., Lei, Y.C., Y.Z. Yang. The roughness and bumping model of cement pavement in seasonal-frost regions. Magazine of Civil Engineering. 2024. 17(1). Article no. 12709. DOI: 10.34910/MCE.127.9

1. Introduction

Roughness is an important pavement characteristic to evaluate the ride quality. Its value has a great impact on driving comfort and safety, damage to roads and vehicles, and is directly related to the amount of maintenance work and the durability of the road. Pavement bumping is a sudden bump of the vehicle caused by damage such as abnormal protrusion or subsidence of the road surface, which not only seriously affects the comfort of the vehicle, but also poses a serious safety hazard to the driving of the vehicle. At the same time, along with greater dynamic load of the vehicle, it causes greater damage to the road surface, decreases the road performance, and increases vehicle wear and fuel consumption. Therefore, in China's

"Highway Performance Assessment Standard" (JTG5210-2018), the pavement bumping index (PBI) is given a certain weight separately, and it is used together with the pavement roughness as an index to evaluate driving comfort.

The research results in China and abroad on pavement roughness and bumping mainly focus on the factors affecting pavement roughness [1], the prediction of pavement roughness [2–4], and the detection and basic control measures of pavement bumping. There is no connection between pavement roughness and bumping, that is why mutual prediction between the two cannot be implemented. Among other studies, research on the factors influencing pavement roughness mainly focuses on the effect of moisture on pavement roughness or the effect of frozen soil environment on pavement roughness [5–9]. Most of the pavement roughness predictions are based on the international roughness index (IRI) prediction model [10–15]. Alimoradi et al. [16] improved the prediction model represented by Markov chain and realized the direct prediction of IRI. Patrick et al [17] considered the effect of different climatic conditions on the susceptibility of pavement to various types of surface distress, and established a relationship between existing surface distress and IRI. Among a few prediction models, the artificial neural network pavement roughness prediction model established by Kargah-Ostadi et al [18] is suitable for flexible pavement in wet-freeze climate, but the application scope is relatively limited. Fang et al [19] used the past roughness index values as alternative indicators of influencing factors to establish a time series pavement roughness prediction model with high accuracy. But since the time series itself is a dynamic tool, the model still needs to be modified. Nurhadiansyah et al [20] proposed to use the gray forecasting model to predict the value of toll road roughness index, and improve forecasting accuracy using Similarity Spatial Data (SSD), but it has higher requirements on the quantity and quality of the data used. At present, pavement bumping is still in the process of improvement. The foreign research on vehicle jumping mostly focuses on vehicle bumps at bridge head and the ways to mitigate these impacts [21, 22]. There are few studies on pavement bumping.

Although the above-mentioned researches are more in-depth regarding the pavement roughness and bumping, the specific relationship between pavement roughness and bumping has not been studied yet, so it is necessary to develop the model of the relationship between pavement roughness and bumping. Establishing a model of the relationship between pavement roughness and bumping in multi-factor conditions can predict them and benefit to improve road safety, driving comfort and timely pavement maintenance.

In order to achieve the goal of establishing a model of the relationship between roughness and bumping on cement pavement suitable for frozen soil and water-rich environment, this study compared the changes in pavement roughness and bumping based on actual survey data of cement roads in frozen soil and water-rich environments, and established a model of the relationship between pavement roughness and bumping, and determined applicable model conditions through experiments.

2. Methods

2.1. The influence of factors on pavement roughness and bumping

In order to explore the effect of frozen soil environment on pavement roughness, China Jing-kun Expressway (K353-K400) (A) and China Ha-zhao Highway (K50-K120) (B) were selected. In order to analyze the effect of frozen soil environment on pavement bumping, China national G214 highway (K97-K720) (C) in Qinghai Province was selected, which includes both non-frozen soil and frozen soil areas. To study the effect of water-rich environment on pavement roughness, China Jing-kun Expressway (K353-K400) (A) and Guangdong Shan-zhan Expressway Zi-jin link section (D) were selected. In order to measure the effect of water-rich environment on pavement bumping, China River Beijing-Harbin Expressway (K102-K262) (E) and Beijing-Hong Kong-Macau Expressway (K1016+000-K1310+000) (F) were selected. In the following discussion, the influence of frozen soil and water-rich conditions on pavement roughness will be divided into left and right sections for consideration. The above expressways were selected based on the location distribution of the seasonal frost regions that have been fully considered.

In order to study the effect of frozen soil environment on pavement roughness. Separate sections A and B, with the standard of separation being the corresponding station numbers every 100m, and assign station numbers 1-8. The laser profiler was used to determine the elevation of the section, and IRI value was synchronized, and the pavement riding quality index (RQI) was calculated using the equation (7.4.7) in Chinese "Highway Performance Assessment Standard" (JTG5210-2018). The result is shown in Fig. 1.

In this figure “Serial number” should be replaced with “Pile number” (as in Figure 1 in the article “Antiskid prediction model for cement pavements in seasonal frost regions”).

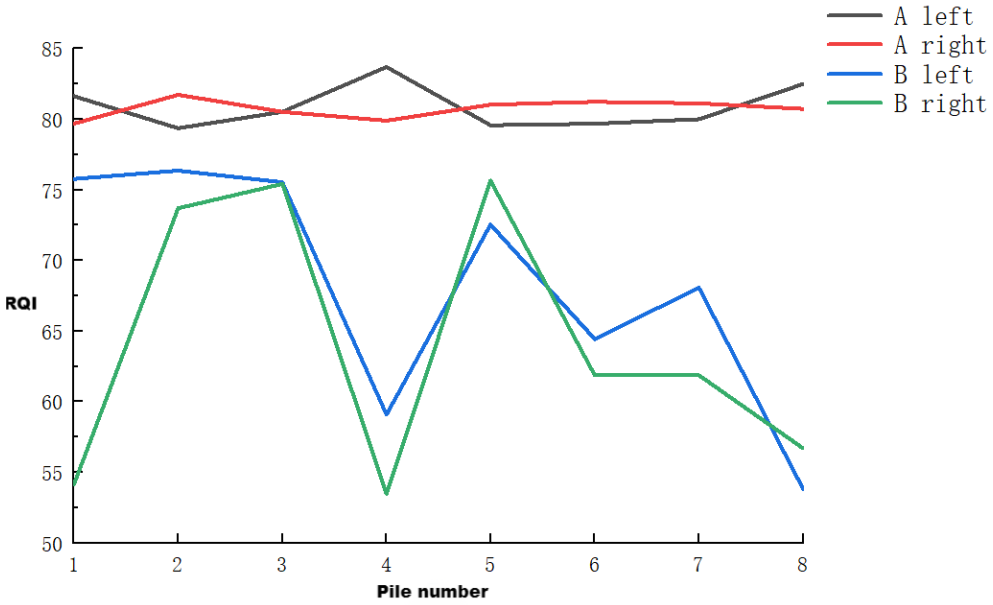

Figure 1. Distribution of pavement roughness in frozen and non-frozen soil areas.

As shown in Fig. 1, the difference between the maximum and minimum values of RQI on the left and right sections of road B in the frozen soil area can reach 20, and the variation is obvious. This is because the right side of the road is adjacent to a sand mining village. The plant uses many heavy-duty vehicles, which largely effects the pavement roughness on the right side of the road. RQI of the left and right sections of road A in the non-frozen soil area averages 82 with slight deviations, which proves that the impact of traffic load on pavement roughness is small. However, if we compare the left section of road A with the left section of road B, the right section of road A and the right section of road B, it becomes obvious that the difference in RQI between road B in the frozen soil area and road A in the non-frozen soil area can reach up to 25. On the left section of road A and the left section of road B at piles 2-3 and 5, the gap varies within 10 %. The main reason for this difference is that the low temperature in the frozen soil area causes the water in the base layer to freeze and solidify, while causing the road surface to expand and swell, at the same time, due to the inconsistent thermal conductivity of the pavement materials, the overall lateral force of the road is uneven. On the left section of road A and the right section of road B at piles 4 and 8, the difference in RQI between road B in frozen soil area and road A in non-frozen soil area is 30. The reason for this is that the water content and ice accumulation of the road sections corresponding to pile numbered 4 and 8 in the seasonal frost area differ from those corresponding to other piles, resulting in uneven frost heaving of the road surface. With the expansion of the frost heave range, the tensile force on the pavement gradually increases. When the tensile limit of the pavement material is exceeded, longitudinal cracks occur, and after the condensed ice melts, the base layer softens and turns into mud. The laitance is squeezed out of the road surface after being crushed by the load of vehicles, causing the road surface to tumble and sink, resulting in drastic changes in the pavement roughness of the road surface.

In order to analyze the impact of frozen soil environment on pavement bumping, using to the above method of dividing the road surface into sections with numbered piles, road C was divided into 44 sections with numbered piles. Moreover, 22 numbered piles were used for the non-frozen soil area and 22 numbered piles were used for the frozen soil area. In order to facilitate comparison of the number of pavement bumping in the frozen and non-frozen soil areas, the non-frozen soil and frozen soil pile numbers are numbered from 1 to 22, respectively. The multi-functional road condition rapid detection system is used to detect the elevation of the vertical section of the road, and determine the presence of bumping and the number of bumps based on the vertical section height difference. The results are shown in Fig. 2.

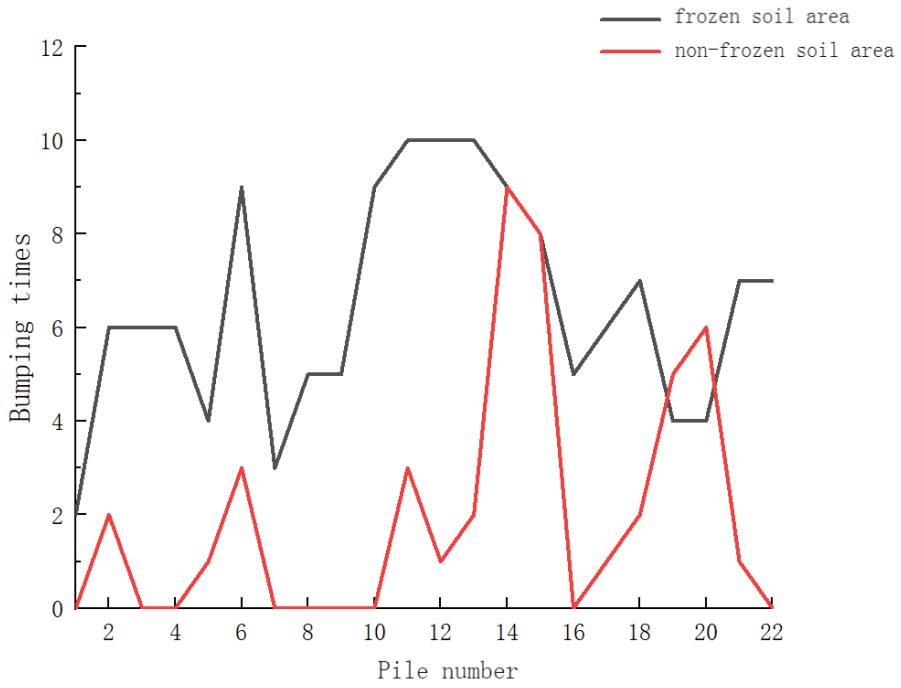

Figure 2. Distribution of pavement bumping in the frozen and non-frozen soil areas.

As shown in Fig. 2, there is a pavement bumping phenomenon in each section of the frozen soil area, and the number of pavement bumping in the frozen soil area is on average greater than that in the non-frozen soil area. Data analysis shows that the number of pavement bumping per kilometer in frozen soil area is about 2.4 times that of non-frozen soil area. The analysis of the cause is that the freezing of soil water and the thickening of ice in the frozen soil area lead to soil expansion and uneven surface uplift. At the same time, the frozen soil sinks when it melts, which eventually leads to uneven settlement of the road surface. Significant changes in road elevation have led to a significant increase in vehicle jumping onto the road while driving. Based on the analysis of Fig. 1 and 2, it is clear that climatic conditions in the seasonal frost regions will lead to the development of a tendency to deteriorate due to pavement roughness and bumping.

To study the effect of water-rich environment on pavement roughness, roads A and D were also divided into sections with piles numbered from 1 to 8. A high-precision profile meters were used to collect elevation data and pavement roughness values. RQI was calculated using the equation (7.4.7) in Chinese "Highway Performance Assessment Standard" (JTG5210-2018). The result is shown in Fig. 3.

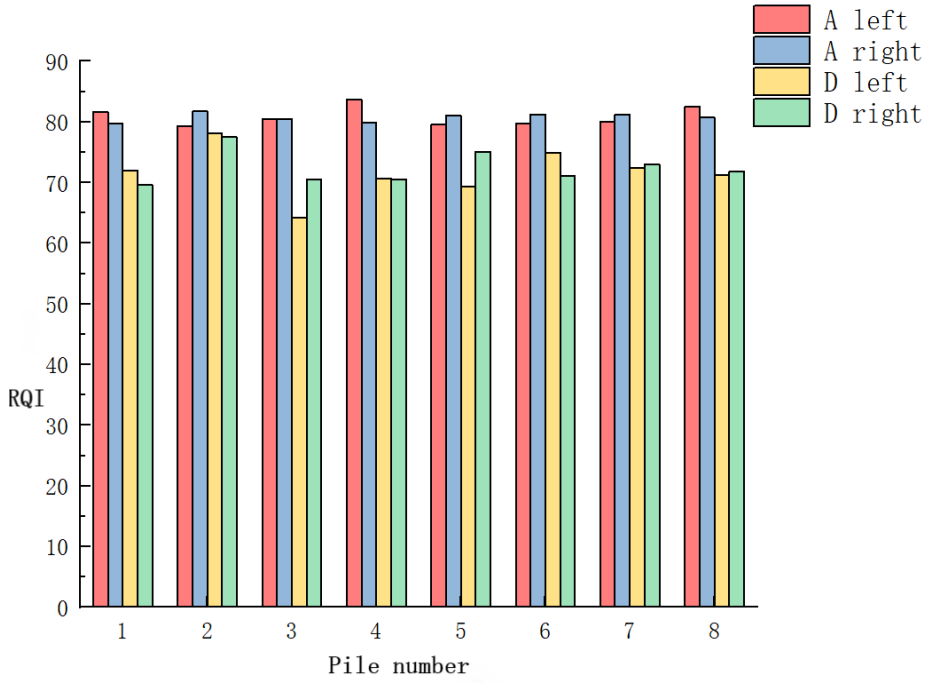

Figure 3. Distribution of pavement roughness in water-rich and non-water-rich areas.

As shown in Fig. 3, RQI of the left and right sections of road A in the non-water-rich area averages 82 with slight deviations, while RQI of the water-rich area averages 70. The reason is that there is a lot of rainfall in the water-rich areas, and the road surface joint filler fails due to rain erosion. With the frequent impact of wheels, the bending tensile stress in the slab exceeds the ultimate flexural strength of the material, resulting in cracks and fractures in the panel. Water infiltrates from the joints or cracks, and the mud in the cracks is squeezed out by the water pressure, causing rainwater to seep between the underlying and base layer. Water pressure becomes too high, and the top ash of the base layer sprays out from the cracks in the road. The base material forms a cavity, which aggravates the pavement network crack. RQI of the left section of road D has a sudden change from 78 to 65 at piles 2 and 3. The reason is that there is groundwater at this piles, and there are cavities in the roadbed soil due to groundwater erosion, which causes the roadbed to sink. At the same time rainwater will be further immersed into the roadbed, and the water content of the roadbed will increase, which will affect the compaction and bearing capacity of the soil. The uneven distribution of the water content of the roadbed soil results in uneven strength of the roadbed, causing local differential settlement of the roadbed, various slope cracks, slope settlement, etc. which lead to sudden changes in pavement roughness. The above analysis shows that water-rich environment has a serious effect on the pavement roughness, and the performance of reducing the pavement roughness is obvious.

To study the effect of water-rich environment on pavement bumping, roads E and F were also divided into sections with piles numbered from 1 to 8. A laser profiler was used to measure longitudinal elevation of the road section. PBI was calculated using the equation (7.4.9) in Chinese "Highway Performance Assessment Standard" (JTG5210-2018). The result is shown in Fig. 4.

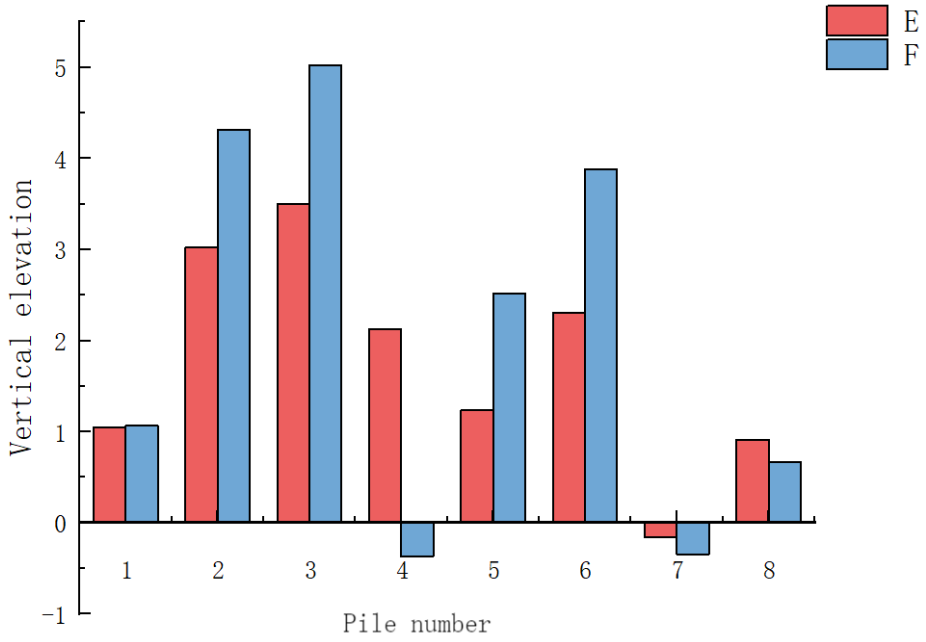

Figure 4. Distribution of pavement bumping in water-rich and non-water-rich areas.

As shown in Fig. 4, the vertical elevation of road E in the non-water-rich area is lower than that of road F in the water-rich area. The road elevation of the road F at the piles 3 and 6 drops significantly. Because the elevation zero point is chosen differently, the phenomenon of changing from positive to negative appears. The reason is that the water content of the roadbed increases due to the large amount of precipitation on road F, which affects the strength of the roadbed and causes the road surface to settle and the phenomenon of pavement bumping to appear. The greater the rainfall, the greater the water content of the roadbed, and the greater the impact on the strength of the roadbed, the greater the road subsidence, the more bumping times will appear.

Based on the analysis of Fig. 3 and 4, it can be concluded that water-rich environment will reduce the roughness of cement concrete pavement and the performance of pavement bumping.

In order to further analyze the impact of the coupling effect of frozen soil and water-rich conditions on the pavement roughness, the data in Fig. 1 and Fig. 3 were summarized, and the results are shown in Fig. 5.

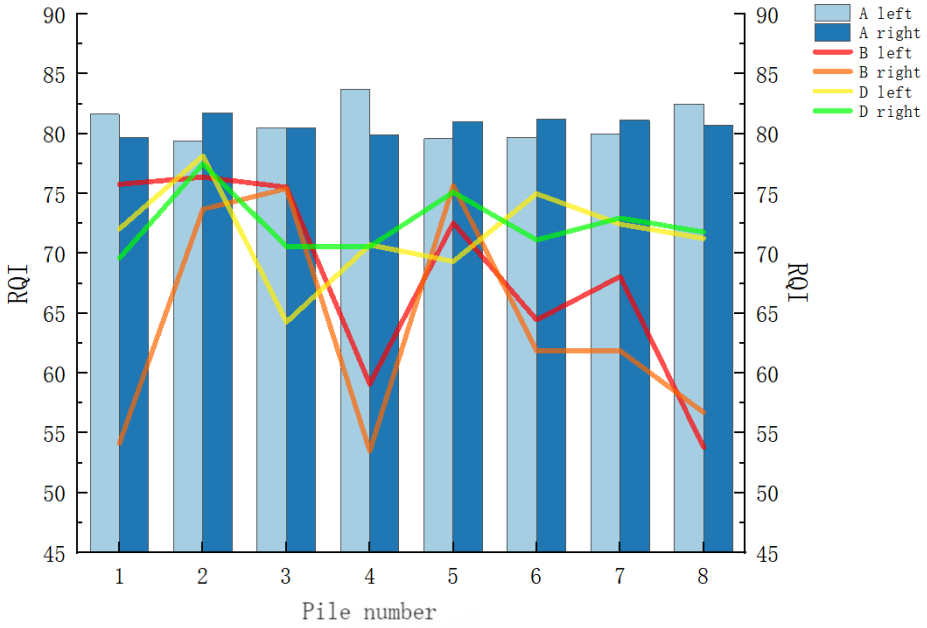

Figure 5. Distribution of road pavement roughness under coupling.

In Fig. 5 RQI of road A in the non-frozen soil and non-water-rich environment averages 80, while RQI s of road B and D in the frozen soil and water-rich environment have decrease significantly. The reason is that under the condition of a certain water content, the lower the temperature, the stronger the frost heave of the soil, the greater the change in road elevation and the smaller RQI is. Under the condition of a certain temperature, the higher the water content, the stronger the frost heave of the soil, the higher the heat resistance and thawing, the greater the change in road elevation and the smaller RQI is. The analysis shows that RQI is directly proportional to temperature and inversely proportional to water content.

In order to explore the impact of frozen soil and water-rich environment on the pavement bumping, the number of severe bumps on the road sections was collected through the road management office of each section and coded 1-8, respectively. The results are shown in Fig. 6.

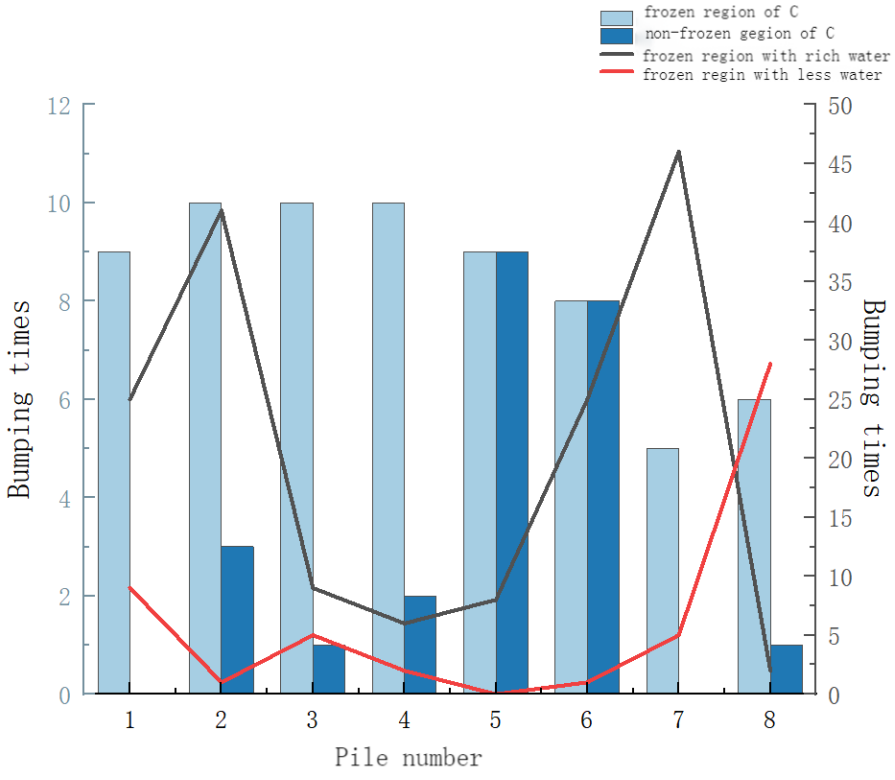

Figure 6. Distribution of pavement bumping under the coupling effect.

As shown in Fig. 6, the number of bumps on the road C and frozen soil areas in the water-rich and frozen soil environment has increased significantly. The reason is that under the condition of a certain water content, the lower the temperature, the stronger the frost heave of the soil, the greater the change in road elevation and the greater the number of bumps is. Under the condition of a certain temperature, the higher the water content, the stronger the frost heave and thaw settlement of the soil, the greater the change in road elevation and the greater the number of bumps is. The analysis shows that bumping times is inversely proportional to temperature and directly proportional to water content.

Combined with the previous analysis, the coupling effect of frozen soil environment and water-rich conditions has a significant impact on pavement roughness and bumping, and the roughness and bumping show a tendency to worsen under frozen soil environment and water-rich conditions. It shows that the roughness of cement concrete pavement has a large correlation with pavement bumping. For further verification, correlation analysis is required.

2.2. Establishment of Model Relationship

According to the above analysis, the indices needed to construct the model relationship between pavement bumping and pavement roughness should include RQI, PBI, frozen soil and water-rich environmental factors. In [23] IRI prediction revised model of cement pavement in frozen season was constructed using MEPDG and in [24] the evaluation indicator for moisture condition in the system of climatic evaluation indicators for highway was proposed. After the processing, the prediction model for pavement bumping and roughness index was established as follows:

$$RQI = K + C_1 \times PBI + C_2 \times t\left(1+0.5556f\right)\left(1+P_{200}\right)\times 10^{-6} + C_3 \times \frac{P}{PE}, \quad (1)$$

where RQI is the pavement riding quality index; PBI is the pavement bumping index; P is the precipitation; PE is the evaporation; $\frac{P}{PE}$ is the water-rich environment factor; t is the service life of the road; f is the freezing index; P_{200} is the passing rate of roadbed materials when the screen hole is 0.075 mm; $t\left(1+0.5556f\right)\left(1+P_{200}\right)\times 10^{-6}$ is the environmental factor of frozen soil; K is a constant; C_1, C_2, C_3 are the corresponding weights.

Since equation (1) is a nonlinear equation, in order to simplify the method and steps of nonlinear equation in regression analysis, the logarithmic function method is used to linearly transform the equation.

Let: $t\left(1+0.5556f\right)\left(1+P_{200}\right)\times 10^{-6} = \alpha$; $\frac{P}{PE} = \beta$.

Then equation (1) can be converted into:

$$RQI = K + C_1 \times PBI + C_2 \times \alpha + C_3 \times \beta. \quad (2)$$

Therefore, the original nonlinear equation can be transformed into a linear equation for solving.

According to the road condition inspection evaluation and maintenance decision analysis report of the main highways in Heilongjiang Province, which involved RQI and PBI of 145 typical road sections in the seasonal freezing area and the rich water area, re-selected the field survey data of 20 highway sections such as Zhaodong, Qiqihar, Mudanjiang. Use the Statistical Package for Social Sciences (SPSS) software to perform regression analysis, combined with formula (2), set RQI measured on the spot as the dependent variable. t, f and P_{200} correspond to the transformed α. P and PE correspond to the transformed β. And the measured PBI on the spot are the independent variables, and the linearity test of the model is carried out. The Analysis Of Variance (ANOVA) of the regression model obtained is shown in Table 1.

In Table 1, the regression sum of squares of the dependent variables is 145.123, and the ratio of the squared sum of the regressions of the factors to the degrees of freedom (the mean square) is 48.374, which is much higher than the mean squared residual 0.238. The ratio of the mean regression squared to the sum of the squared mean residuals (F) is 202.986. The value is large, indicating that the change of the dependent variable is caused by the change of the independent variable rather than the experimental error, and the independent variable has a high explanatory force for the dependent variable. The significance

value is 0, less than 0.05, the model linear regression is significant. It shows that in the F test, the linear regression of the equation is obvious, and a linear model can be established between the dependent variable and the independent variable.

Table 1. Regression model of ANOVAs.

	Sum of squares	Degree of freedom	Mean square	F	Significance
Regression	145.123	3	48.374	202.986	0
Residual	3.813	16	0.238		
Total	148.936	19			

After the F test shows that a linear model can be established, it is necessary to determine whether the independent variable has a significant influence on the dependent variable, so the regression coefficients should be tested for significance. The partial regression coefficient in Table 2 represents the weight of each index. The absolute value of the standardized partial regression coefficient indicates the degree of influence of each variable on the dependent variable. The absolute value of the standardized partial regression coefficient of α is the largest among the three indicators, indicating that α corresponds to the parameters t, f and P_{200} have the greatest impact on the RQI value. The parameters P and PE correspond to β, and the relatively small impact is PBI, which is consistent with the results of the analysis of variance when determining the relations between the parameters and RQI. The absolute value of the partial regression coefficient of α is 5431.712. The reason for the analysis is that the value of the frozen soil environmental factor $t\left(1+0.5556f\right)\left(1+P_{200}\right)\times10^{-6}$ is small, so the weight in the model is relatively large. The absolute value of the critical value *t* of the bilateral test is all-greater than the significance level, indicating that the independent variable has a significant influence on the dependent variable, and all the independent variables are retained in the model.

Table 2. Coefficient of regression modelю

Parameter	Partial regression coefficient	Partial regression coefficient standard error	Standardized partial regression coefficient	t	Significance
Constant	104.403	3.997		26.122	0
α	–5432.712	332.731	–0.931	–16.328	0
PBI	–0.070	0.038	–0.087	–1.826	0.087
β	–0.123	0.070	–0.112	–1.752	0.099

Bringing the results of the above regression analysis into equation (2), the model is expressed as:

$$RQI = 104.403 - 0.07 \times PBI - 5432.712\alpha - 0.123\beta. \quad (3)$$

Reconverted to a nonlinear equation:

$$RQI = 104.403 - 0.07 \times PBI - 5432.712t\left(1+0.5556f\right)\left(1+P_{200}\right)\times10^{-6} - 0.123\frac{P}{PE}. \quad (4)$$

After the prediction model of the relationship between pavement bumping and pavement roughness is established, the goodness of fit between the independent variable and the dependent variable should be tested to ensure that the dependent variable can be interpreted by the model. In Table 3, R^2 is the deterministic coefficient between the dependent variable and the independent variable. Adjusted R^2 is the mean square error ratio that eliminates the influence of the number of independent variables. The closer R^2 and adjusted R^2 are to 1, the better the fitting effect of the regression equation. The adjusted R^2 of the regression equation is 0.970, which is close to 1, and the standard estimation error is 0.488, indicating that the model has a high degree of goodness of fit and the dependent variable can be explained by the model accounting for 95 %.

Table 3. Summary of regression models.

R2	Adjusted R2	Standard estimation error
0.974	0.970	0.488

In order to verify the applicability of the prediction model of the relationship between pavement bumping and pavement roughness, the normal distribution test was carried out for the model. Observing the residual histogram and the normal distribution curve in Fig. 7, we can see that the sample size is large enough and the residual distribution conforms to the normal distribution, which proves the correctness of the prediction model. Observing the residual regression P-P graph in Fig. 8, the residual distribution curve changes around the preset diagonal and diagonal directions. The two are close to coincide, and the regression model satisfies the normal distribution hypothesis. In summary, the RQI prediction model established by using PBI, t, f, P_{200}, P and PE as parameters has passed various tests, and the regression effect is significant, and the goodness of fit is high.

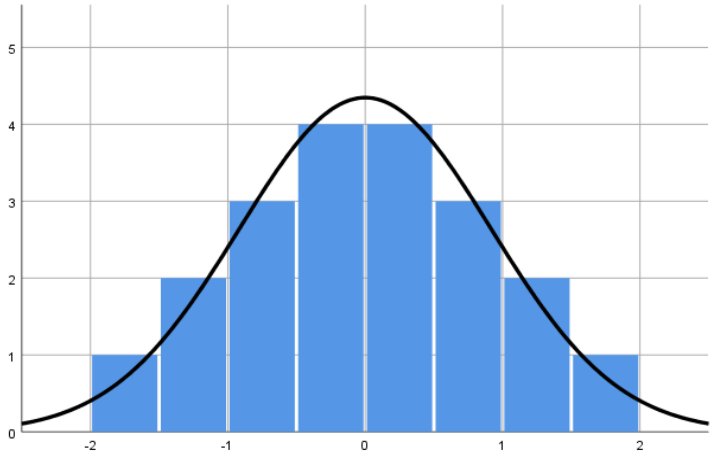

Figure 7. Residual histogram.

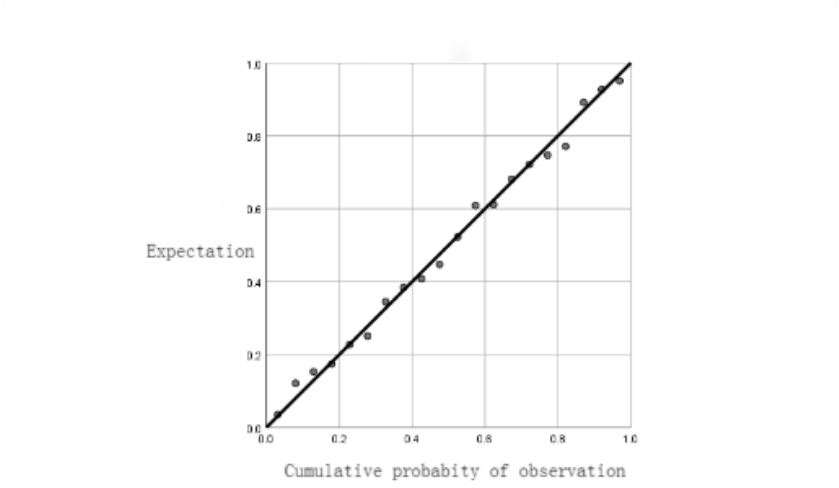

Figure 8. Residual regression P-P graph.

2.3. Analysis of the applicable conditions of the model

In order to ensure high accuracy of model evaluation, a response surface test was designed to determine the optimal prediction space for the cement concrete pavement bumping and pavement roughness prediction model under water-rich environment in the seasonal frost region. In order to facilitate the drawing of test records, the permafrost environmental factors and the water-rich environmental factors in response surface test are replaced by α and β, respectively, and the codes of PBI, α and β are A, B, and C, respectively. According to the number and range of parameters, a response surface test with 3 factors and 3 levels was selected. The coding levels and value are shown in Table 4. In order to simplify the process of drawing the response surface of PBI, α and β to RQI, the ordinate of the response surface is set as RQI value, and the abscissa is the factor value.

Table 4. Coding level table.

Code	Factor name	-1	0	1
A	PBI	87.50	93.75	100.00
B	α	0.0002	0.0010	0.0018
C	β	6.59	10.73	14.87

In the case where the coding level of PBI is 0, the response surfaces of design α and β to RQI value are as shown in Fig. 9a. When β is in the range of 6.59 to 10.73, the inclination of the response surface is smaller than the inclination of 10.73 to 14.87. The reason is that with the increase of β, the higher the moisture content of the subgrade soil, the more groundwater and the stronger the scouring effect of water on the subgrade soil. The strength of the subgrade soil is significantly lower than that of the ground moisture content, so that RQI value is significantly increased compared to the road section with low water-rich factor, so RQI is more responsive to the β range of 10.73 to 14.87.

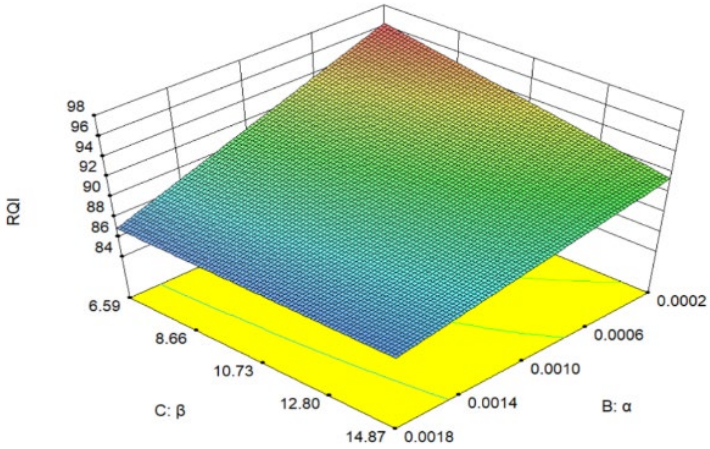

Figure 9a. Response surface of α and β to RQI value.

In the case where the coding level of α is 0, the response surfaces of PBI and β to RQI value are as shown in Fig. 9b. Observing the surface change of PBI in Fig. 9b, the inclination of the response surface increases significantly, when PBI is from 87.5 to 95 compared with that from 95 to 100. The reason is that with the decrease of PBI, the uneven settlement of the road surface becomes more and more serious. The more obvious, the more drastic the change of road elevation, so that RQI value increases significantly compared with the road sections with no obvious changes in road elevation, indicating that RQI is more responsive to PBI range of 87.5 to 95.

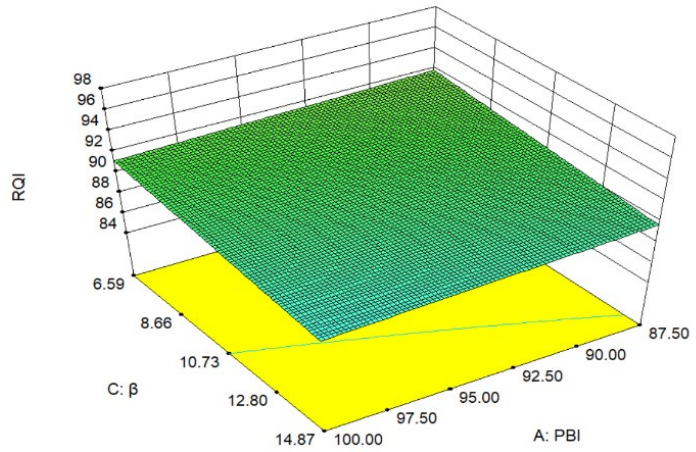

Figure 9b. Response surface of PBI and β to RQI value.

In the case where the coding level of β is 0, the response surfaces of PBI and α to RQI values are as shown in Fig. 9c. Observing the surface change of α in Fig. 9c, with the increase of α, the frost heave and thawing properties of the subgrade soil increase, and RQI value decreases accordingly. When α is from 0.0002 to 0.0014, the slope of the surface is larger than that from 0.0014 to 0.0018, and RQI value is significantly reduced. Obviously, therefore RQI has the highest responsivity to α in the range from 0.0002 to 0.0014.

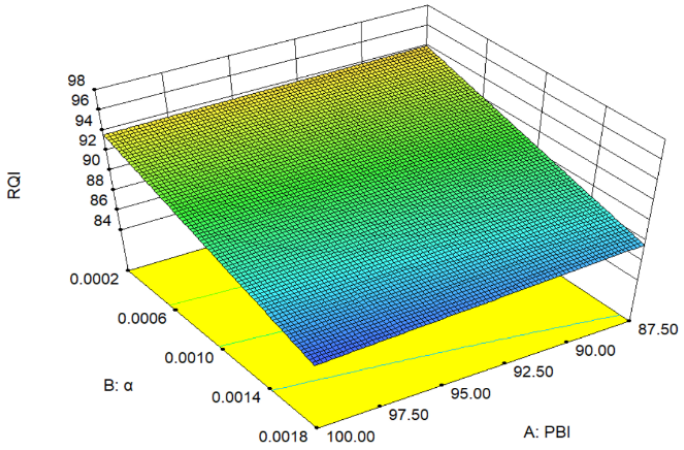

Figure 9c. Response curves of PBI and α to RQI value.

Combined with the response surface analysis above, it can be seen that the response surface tends to be flat. It means that within the range of parameters corresponding to the surface, RQI value cannot change synchronously with the parameter value, and RQI is more responsive to the parameter change. At this time, the prediction accuracy of the cement concrete pavement bumping and pavement roughness prediction model is low. If the slope of the response surface is large, RQI value changes significantly, and the corresponding parameter range is more suitable for model prediction. According to the results of the response surface analysis, the optimal prediction space of the model is the parameter value range when PBI is from 87.5 to 95, the permafrost environmental factor is from 0.0002 to 0.0014, and the water-rich environmental factor is from 10.73 to 14.87. When the optimal prediction space is selected, the prediction level of the model is the best.

3. Results and Discussion

In order to verify the practicability of the cement concrete pavement bumping and pavement roughness prediction model under the water-rich conditions in the seasonal frost region, the measured value of RQI and the predicted value of the model in 20 highway sections including Daqing and Heihe were selected for verification. The Statistical Package for Social Sciences (SPSS) Statistics software suit was used. The predicted value is matched with the measured value of RQI, as shown in Fig. 10. In Fig. 10, the abscissa is the measured value of RQI, and the ordinate is the predicted value of RQI. It can be seen from the figure that the scattered points corresponding to the measured value and the predicted value are evenly distributed on both sides of the straight line and are close to the straight line. The deterministic coefficient R^2 of the fitting between the predicted value of the prediction model RQI and the measured value is 0.987, which proves that the prediction model has a high degree of fit.

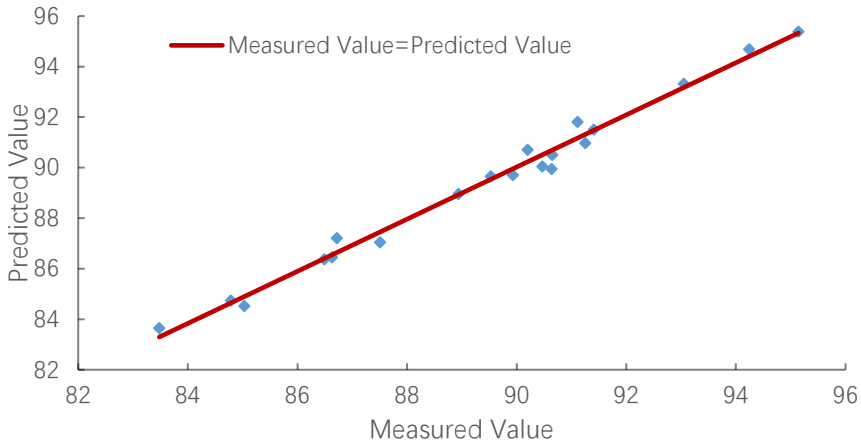

Figure 10. Correlation fitting between RQI predicted value and measured value.

In order to further reflect the fitting effect of the prediction model, separately count the prediction values of the cement concrete pavement roughness and bumping prediction model, the Backpropagation (BP) neural network prediction model [25] and the Logistic model [26–32] under the water-rich condition in the seasonal frost region. The difference between the predicted value and the actual value is shown in Fig. 11. It can be seen from Fig. 11 that the difference between the actual measured value and the predicted value of the cement concrete pavement roughness and bumping prediction model under the water-rich condition in the seasonal frost region is concentrated within ±0.5. And the BP neural network prediction model is distributed between ±0.75. The Logistic model is distributed between ±1.5. It proves that the prediction model is closer to the true value than the prediction results of the BP neural network prediction model and the Logistic model, and the prediction model has better effects and better practicability.

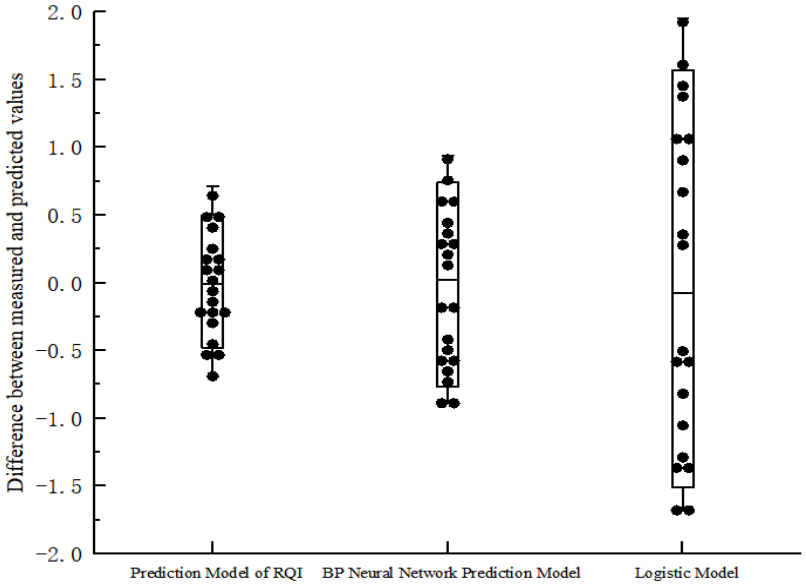

Figure 11. The prediction error of the model.

4. Conclusions

1. Frozen soil conditions and water-rich conditions will change the pavement roughness in a negative direction, and at the same time will cause the number of pavement bumping to change in a positive direction. In areas with no frozen soil and water-rich conditions, the pavement riding quality index (RQI) averages 80, while RQI in water-rich areas averages 70. In frozen soil and non-frozen soil areas the difference in RQI can reach 25. At the same time, the number of pavement bumping per kilometer in the permafrost area is 2.4 times that of the non-frozen soil area. The road elevation in the water-rich area has a sudden change from positive to negative, which is more drastic than in the non-water-rich area.

2. Frozen soil and water-rich factors are the key factors that affect the pavement roughness and pavement bumping in the water-rich conditions in seasonal frost regions. The absolute values of the standardized partial regression coefficients of frozen soil environment and water-rich environment factors are 0.931 and 0.112, respectively, indicating that the freezing index of frozen soil environment factors has the most significant effect, followed by precipitation in water-rich environment.
3. The relationship model between pavement roughness and bumping under the conditions of rich water in seasonal frost regions is proposed, using four factors, including RQI, pavement bumping index (PBI), frozen soil environmental factors and water-rich environmental factors. It can predict the pavement roughness and bumping of cement concrete pavement under water-rich conditions in seasonal frost region. The prediction model is a composite function. The deterministic coefficient R^2 of the prediction model is 0.970, and the significance level is 0. The model has a high degree of fit and significant regression. It shows that the prediction model has statistical applicability.
4. When PBI is from 87.5 to 95, the permafrost environmental factor is from 0.0002 to 0.0014, and the water-rich environmental factor is from 10.73 to 14.87, the response of RQI to parameter changes is higher than that of other parameters, which is the optimal prediction space of the model. At this time, the prediction level of the model is the best.
5. Prediction models for pavement roughness and bumping under water-rich conditions in seasonal frost regions have good accuracy. Through the verification of the prediction model in different periods of the same road section and the same period of different road sections, the R^2 of the prediction model is 0.987, and the difference between the predicted value and the measured value is within ±0.5. Compared with the BP neural network prediction model and the Logistic model, it shows a strong prediction accuracy.

References

1. Ali, A., Dhasmana, H., Hossain, K., Hussein, A. Modeling Pavement Performance Indices in Harsh Climate Regions. Journal of Transportation Engineering, Part B: Pavements. 2021. 147 (4). DOI: 10.1061/JPEODX.0000305
2. Wang, K.C.P., Li, Q., Hall, K.D., Elliot, R.P. Experimentation with gray theory for pavement smoothness prediction. Transportation Research Record: Journal of the Transportation Research Board. 2007. 1990 (1). Pp. 3–13. DOI: 10.3141/1990-01
3. Múčka, P. Current approaches to quantify the longitudinal road roughness. International Journal of Pavement Engineering. 2016. 17 (8). Pp. 659–679. DOI: 10.1080/10298436.2015.1011782
4. Soncim, S.P., de Oliveira, I.C.S., Santos, F.B., Oliveira, C.A. d. S. Development of probabilistic models for predicting roughness in asphalt pavement. Road Materials and Pavement Design. 2018. 19 (6). Pp. 1448–1457. DOI: 10.1080/14680629.2017.1304233
5. Miao, Y.-H., Wang, B.-G., Li, C., Gupta, P.K. Climate zoning for moisture damage of asphalt pavements in China. Journal of Chang'an University: Natural Science Edition. 2008. 28 (1). Pp. 26–31.
6. Byrne, M., Albrecht, D., Sanjayan, J.G., J.K. Identifying the effects of soil and climate types on seasonal variation of pavement roughness using MML inference. Journal of Computing in Civil Engineering. 2008. 22 (2). Pp. 90–99. DOI: 10.1061/(ASCE)0887-3801(2008)22:2(90)
7. Bae, A., Stoffels, S.M., Antle, C.E., Lee, S.W. Observed evidence of subgrade moisture influence on pavement longitudinal profile. Canadian Journal of Civil Engineering. 2008. 35. Pp. 1050–1063. DOI: 10.1139/L08-047
8. Sylvestre, O., Bilodeau, J.P., Doré, G. Effect of frost heave on long-term roughness deterioration of flexible pavement structures. International Journal of Pavement Engineering. 2019. 20 (6). Pp. 704–713. DOI: 10.1080/10298436.2017.1326598
9. Bo, L., Kundwa, M.J., Jiao, C.Y., Wei, Z.X. Pavement Performance Evaluation and Maintenance Decision-Making in Rwanda. 3rd GeoMEast International Congress and Exhibition on Sustainable Civil Infrastructures, GeoMEast 2019, November 10–15. Cairo, Egypt. 2020. Pp. 107–116. DOI: 10.1007/978-3-030-34196-1_8
10. Sun, L. Simulation of pavement roughness and IRI based on power spectral density. Mathematics and Computers Simulation. 2003. 61 (2). Pp. 77–88. DOI: 10.1016/S0378-4754(01)00386-X
11. Park, K., Thomas, N.E., Lee K.W. Applicability of the international roughness index as a predictor of asphalt pavement condition. Journal of Transportation Engineering. 2007. 133 (12). Pp. 706–709. DOI: 10.1061/(ASCE)0733-947X(2007)133:12(706)
12. Hossain, M.I., Gopisetti, L.S.P., Miah, M.S. Prediction of international roughness index of flexible pavements from climate and traffic data using artificial neural network modeling. International Conference on Highway Pavements and Airfield Technology 2017, August 27–30. Philadelphia, US. 2017. Pp. 256–267. DOI: 10.1061/9780784480922.023.
13. Li, W., Huyan, J., Xiao, L., Tighe, S., Pei L. International roughness index prediction based on multigranularity fuzzy time series and particle swarm optimization. Expert Systems with Applications: X. 2019. 2. 100006. DOI: 10.1016/j.eswax.2019.100006
14. Abdelaziz, N., Abd El-Hakim, R.T., El-Badawy, S.M., Hafez, A.A. International Roughness Index prediction model for flexible pavements. International Journal of Pavement Engineering. 2020. 21 (1). Pp. 88–99. DOI: 10.1080/10298436.2018.1441414
15. Zhang, L.N., He, D.P., Zhao, Q.Q. Modeling of international roughness index in seasonal frozen area. Magazine of Civil Engineering. 2021. 104 (4). 10402. DOI: 10.34910/MCE.104.2

16. Alimoradi, S., Golroo, A., Asgharzadeh S.M. Development of pavement roughness master curves using Markov Chain. International Journal of Pavement Engineering. 2020. 23 (2). Pp. 453–463. DOI: 10.1080/10298436.2020.1752917
17. Patrick, G., Soliman H. Roughness prediction models using pavement surface distresses in different Canadian climatic regions. Canadian Journal of Civil Engineering. 2019. 46 (10). Pp. 934–940. DOI: 10.1139/cjce-2018-0697
18. Kargah-Ostadi, N., Stoffels, S.M., Tabatabaee, N. Network-Level Pavement Roughness Prediction Model for Rehabilitation Recommendations. Transportation Research Record: Journal of the Transportation Research Board. 2010. 2155 (1). Pp. 124–133. DOI: 10.3141/2155-14
19. Ni, F.-J., Fang, Y., Xue, Z.-M. Prediction of pavement roughness with time series autoregression model. Journal of Southeast University: Natural Science Edition. 2006. 36 (4). Pp. 634–637.
20. Nurhadiansyah, R., Hadiana, A. Toll Road Roughness Index Forecasting with Combination Grey Forecasting Model and Similarity Spatial Data. IOP Conference Series: Materials Science and Engineering. 2019. 662. 022065. DOI: 10.1088/1757-899X/662/2/022065
21. Zhao, H., Hui, Z., Lin, J. Study on soft foundation settlement analysis and treatment of bridge-head. Advanced Materials Research. 2013. 779-780. Pp. 632–635. DOI: 10.4028/www.scientific.net/AMR.779-780.632
22. Tu, Y., Wang, X., Chai, H., Xu, J., Li, H., Yu, J. Effects of jet grouting pile composite foundation with variable stiffness treating vehicle bump at bridge head. Journal of Southeast University: Natural Science Edition. 2021. 51 (4). Pp. 588–595.
23. Zhao, Q., Cheng, P., Wei, Y., Zhou, X. IRI predictive revised model for cement pavement in seasonal frozen region using MEPDG. Journal of Harbin Institute of Technology. 2018. 50 (11). Pp. 171–177. DOI: 10.11918/j.issn.0367-6234.20170056
24. Miao, Y.-H., Wang, B.-G. Research on Climatic Evaluation Indicators for Highway. Journal of Beijing University of Technology. 2007. 33 (11). Pp. 1168–1172+1186.
25. Xu, B., Dan, H.-C., Li L. Temperature prediction model of asphalt pavement in cold regions based on an improved BP neural network. Applied Thermal Engineering. 2017. 120. Pp. 568–580. DOI: 10.1016/j.applthermaleng.2017.04.024.
26. Heidari, M.J., Najafi, A., Alavi, S. Pavement deterioration modeling for forest roads based on logistic regression and artificial neural networks. Croatian Journal of Forest Engineering. 2018. 39 (2). Pp. 271–287.
27. Tasmin, T., Wang, J., Dia, H., Richards, D., Tushar, Q. A probabilistic approach to evaluate the relationship between visual and quantified pavement distress data using logistic regression. 2020 IEEE Asia-Pacific Conference on Computer Science and Data Engineering, December 16–18. Gold Coast, Australia. 2020. Pp. 1–4. DOI: 10.1109/CSDE50874.2020.9411555
28. Kharun, M., Klyuev, S., Koroteev, D., Chiadighikaobi, P.C., Fediuk, R., Olisov, A., Vatin, N., Alfimova, N. Heat treatment of basalt fiber reinforced expanded clay concrete with increased strength for cast-in-situ construction. Fibers. 2020. 8 (11). Pp. 1–16. DOI: 10.3390/fib8110067
29. Fediuk, R., Smoliakov, A., Stoyushko, N. Increase in composite binder activity. IOP Conference Series: Materials Science and Engineering. 2016. 156. 012042. DOI: 10.1088/1757-899X/156/1/012042
30. Prakash, R., Divyah, N., Srividhya, S., Avudaiappan, S., Amran, M., Naidu Raman, S., Guindos, P., Vatin, N., Fediuk, R. Effect of Steel Fiber on the Strength and Flexural Characteristics of Coconut Shell Concrete Partially Blended with Fly Ash. Materials. 2022. 15 (12). 4272. DOI: 10.3390/ma15124272
31. Fediuk, R.S., Smoliakov, A.K., Timokhin, R.A., Batarshin, V.O., Yevdokimova, Yu.G. Using thermal power plants waste for building materials. IOP Conference Series: Earth and Environmental Science. 2018. 87. 092010. DOI: 10.1088/1755-1315/87/9/092010
32. Fediuk, R., Yushin, A. Composite binders for concrete with reduced permeability. IOP Conference Series: Materials Science and Engineering. 2016. 116. 012021. DOI: 10.1088/1757-899X/116/1/012021
33. Fediuk, R.S., Lesovik, V.S., Mochalov, A.V., Otsokov, K.A., Lashina, I.V., Timokhin, R.A. Composite binders for concrete of protective structures. Magazine of Civil Engineering. 2018. 82 (6). Pp. 208–218. DOI: 10.18720/MCE.82.19
34. Fediuk, R.S., Lesovik, V.S., Liseitsev, Yu.L., Timokhin, R.A., Bituyev, A.V., Zaiakhanov, M.Ye., Mochalov, A.V. Composite binders for concretes with improved shock resistance. Magazine of Civil Engineering. 2019. 85 (1). Pp. 28–38. DOI: 10.18720/MCE.85.3

Information about authors:

Hanqing Li,
E-mail: 79549482@qq.com

Qiao Sun,
E-mail: 465390034@qq.com

Zakaria Ideris,
E-mail: ideris753@gmail.com

Qianqian Zhao,
ORCID: https://orcid.org/0000-0002-0209-4181
E-mail: 492954791@qq.com

Roman Fediuk,
ORCID: https://orcid.org/0000-0002-2279-1240
E-mail: roman44@yandex.ru

Yuchuan Lei,
ORCID: https://orcid.org/0000-0001-9556-2951
E-mail: 1371904682@qq.com

Yang Yuze,
E-mail: 18645921558@qq.com

Received: 12.01.2022. Approved after reviewing: 07.02.2024. Accepted: 20.03.2024.